Comparing Emission Estimation Models for Rail Freight Transportation

Arne Heinold

School of Economics and Business, Kiel University, Kiel, Germany

Abstract

This study reviews emission estimation models that aim at providing realistic estimates of the emitted greenhouse gases from rail freight transportation. Five models are considered: two models from the MEET project, the ARTEMIS model, the EcoTransIT World model, and the Mesoscopic model. For each of the five models, this paper describes the estimation principles, methodology, and procedure, as well as relevant input parameters. An experimental study demonstrates the impact of train and trip specific parameters on each model's emission estimate. Results are presented for varying values of a train's number of wagons, the payload per wagon, the average speed, the trip distance, the number of stops, and the altitude profile along the route. In doing so, given a specific transportation scenario, the paper supports decision makers from industry and researchers to find and apply an appropriate emission estimation model for evaluating the eco-friendliness of rail freight transportation.

Keywords: rail freight transportation, emission estimation models, comparative study, experimental study, carbon dioxide emissions

Email address: arne.heinold@bwl.uni-kiel.de (Arne Heinold)

July 29, 2020

1. Introduction

There is a recent revival of using rail transportation to match the constantly increasing global freight volume (International Energy Agency, 2019). The International Transport Forum (2019) expects global rail freight volumes to grow 2.7% per year between 2015 and 2030, with some countries having significantly higher growth rates (e.g., in 2017, growth rates are 13.3%, 6.4%, 5.5.%, and 5.2% for China, Russia, India, and the USA, respectively). Recent infrastructural developments demonstrate this growth, such as the 'silk railway' initiated by the Chinese government to reduce transportation time between China and Europe (The Times, 2020). Further, transportation makes up for about 25% of global energy-related CO_2 emissions (Eurostat, 2020; IPPC, 2018) and the rail mode is often considered as a mean to reduce total emissions from transportation. For example, recent studies show that using intermodal rail/road transportation instead of road-only transportation can reduce the overall transport emissions, e.g., Craig et al. (2013), Kiyota et al. (2015), de Miranda Pinto et al. (2018), or Heinold and Meisel (2018, 2019). These studies analyze different transport scenarios and apply diverse emission estimation models to measure the environmental impact of the considered modes of transportation. Demir et al. (2011) provide a comparative analysis of several vehicle emission models for road freight transportation. As far as is known, there is no such analysis of emission estimation models for rail freight transportation.

This study fills this gap by reviewing and comparing five emission estimation models for rail freight transportation. The selected models provide an overview of the most common emission estimation approaches. For this, two models from the MEET project (Hickman et al., 1999), the ARTEMIS model (Lindgreen and Sorenson, 2005a,b), the EcoTransIT World (ETW) model (EcoTransIT World Initiative, 2019), and the Mesoscopic model (Kirschstein and Meisel, 2015) are considered in this study. In a first step, each model's estimation principles, methodology, input parameters, and procedures are explained. Then, in a second step, the impact of varying values of a train's number of wagons, the payload per wagon, the average speed, the trip distance, the number of stops, and the altitude profile along the route is demonstrated in an experimental study. Here, a typical freight train serves as a base scenario and results are presented for each of the considered experimental settings, which results in emission rates for a large amount of potential

transport scenarios. Finally, in a third step, this paper discusses scenarios in which it might be appropriate to select one or another of the considered models.

With this, the main contribution of this paper is twofold. Firstly, the models' detailed description with a consistent notation allows a direct and precise application of the models. All models are implemented in Python and the code is made publicly available, see Appendix A. Secondly, the results of the experimental study demonstrate the impact of relevant train and trip specific parameters on each model's emission estimate. In doing so, given a specific transportation scenario, the paper supports decision makers from industry and researchers to find and apply an appropriate emission estimation model for evaluating the eco-friendliness of rail freight transportation.

The rest of this paper is organized as follows. Section 2 describes general principles of estimating emissions from rail freight transportation. Section 3 describes each of the considered emission estimation models in detail. The experimental study in Section 4 demonstrates the impact of train and trip parameters on each model's emission estimate. Section 5 discusses the selection of an appropriate model for a given transport scenario. Section 6 concludes this paper.

2. Principles of estimating emissions from rail freight transportation

This section describes the fundamental principles of estimating emissions from rail freight transportation. Here, emissions refer to all greenhouse gases that result from the combustion of fuel and electricity to power freight transport equipment, most notably, carbon dioxide (CO_2), nitrogen oxides (NO_x), sulfur dioxide (SO_2), and non-methane hydrocarbons (NMHCs). These gases are subsumed under the single measure of carbon dioxide equivalents (CO_2e) that is then used to measure transport related emissions, see Piecyk et al. (2012). Generally, transport related emissions can be distinguished by their life-cycle phase, which refers to either well-to-tank (WTT), tank-to-wheel (TTW), or well-to-wheel (WTW) emissions (e.g., Moro and Lonza, 2018). Well-to-tank emissions include all emissions that are emitted in the production and distribution of the used energy source, such as emissions at power plants or emissions from tank trucks that refuel gas stations. In contrast, tank-to-wheel emissions describe the instant emissions from the energy that is required to move the considered vehicle. Typically, for diesel trains, these are emissions from

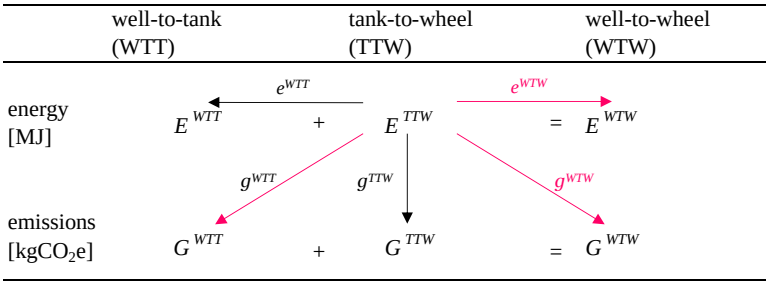

Figure 1: Structure of estimating energy and emissions from rail transportation.

burning the used type of fuel. Finally, well-to-tank and tank-to-wheel emissions add up to well-to-wheel emissions. Note that, in carbon accounting, emissions are further differentiated according to their scope (GHG Protocol, 2020, p. 25), which, however, is not considered in this study.

For each phase (WTT, TTW, and WTW), it is possible to estimate the energy and emissions of a train on a specific trip. Furthermore, by using so-called energy and emission factors, a distinct relation between each phase's energy and emission estimate can be drawn. Figure 1 demonstrates this by using the definition of these factors that is also used in European norm DIN EN 16258 (2012). In particular, TTW emissions G^{TTW} ($kgCO_2e$) are calculated from the actual TTW energy E^{TTW} (MJ) consumed by the train and emission factor g^{TTW} ($kgCO_2e$/MJ) and, likewise, energy and emission factors e^{WTW} (MJ/MJ) and g^{WTW} ($kgCO_2e$/MJ) can be directly applied to the TTW energy E^{TTW} for calculating WTW energy and emissions, respectively. Finally, it is also possible to derive the WTT energy and emissions from the TTW energy consumption, by applying energy and emission factors e^{WTT} (MJ/MJ) and g^{WTT} ($kgCO_2e$/MJ), respectively. Here, artificial energy factor e^{WTT} shows the energy in the production and distribution processes per unit of energy that is required to move the train. For several train and engine types, these emission and energy factors are provided by the literature. If this is the case, a train's emissions and energy can be derived solely from its TTW energy consumption. Thus, most emission estimation models, including the ones considered in this study, present a methodology to estimate the TTW energy consumption.

3. Emission estimation models

Emission estimation models usually follow a microscopic or a macroscopic approach. The former is based on a detailed consideration of the underlying physical principles of the moving ve-

hicle and the latter is primarily based on aggregated statistical data of the transportation process. So-called mesoscopic models rely on a mixture of micro- and macroscopic principles. This paper considers models from each of the three approaches (micro-, macro-, and mesoscopic) and, with this, it provides a comprehensive overview of commonly used approaches for estimating emissions. Thereby, early seminal models (MEET from 1999, ARTEMIS from 2005) and recent, more practically oriented models (global ETW from 2010, Mesoscopic from 2015) are explained in this section. The models analyzed in this study are presented in the order of their year of publication (oldest to newest). Table 1 provides the notation for the trip's distance, the trip's altitude difference, the train's weights, the train's number of wagons and axles, the trip's number of stops, and the train's average speed. This notation is consistently used across all the considered models and further notation that is specific the models is introduced in the respective subsections.

3.1. MEET

Hickman et al. (1999) present Methodologies for Estimating Emissions from Transport (MEET). The work provides estimation models for road, rail, sea, and air transportation of passengers and freight. For rail transportation, the general idea is to estimate a TTW-energy consumption rate in kJ per ton and kilometer with an estimation function that is parameterized with empirical or train specific data. This rate is then used to calculate the train's total energy consumption through considering the train's payload and the traveled distance. The MEET project proposes two models

Table 1: Consistent notation of common trip and train parameters.

parameter	description	unit
d	trip's distance	m or km
h	trip's altitude difference	m
m_{loc}	train's locomotive weight	kg or ton
m_t	train's total weight	kg or ton
m_{tl}	train's payload	kg or ton
m_{te}	train's empty weight	kg or ton
m_w	wagon's total weight	kg or ton
m_{we}	wagon's empty weight	kg or ton
m_{wl}	wagon's payload	kg or ton
m_{wm}	wagon's max. payload	kg or ton
n_{ax}	wagon's number of axles	-
n_w	train's number of wagons	-
n_s	trip's number of stops (excl. last stop)	-
v	train's average speed	m/s or km/h

for estimating energy consumption rates.

The first model, also referred to as the empirical MEET model, describes the energy consumption rate as a function of the train's average speed v and the distance d_s between two stops. Formula (1) shows the estimation of the energy per ton and kilometer for a large freight train if the distance between two stops d_s is between 80 and 200 kilometers. Here, A_0 and A_1 are train type specific parameters that were derived from an empirical study.

$$\overset{[kJ/ton\cdot km]}{E_1} = \overset{[-]}{A_0} + \overset{[-]}{A_1} \cdot \frac{\overset{[km/h]^2}{v^2}}{\ln(\overset{[km]}{d_s})}, \; d_s \in [80, 200] \tag{1}$$

The second model, also referred to as the steady state MEET model, derives the train's energy consumption rate from its steady state loading, see Formula (2). Here, the rate is calculated from average speed v, number of stops n_s, distance d, maximum speed v_{max}, and gradient h. Note that v is the train's average speed and v_{max} its maximal speed to which it accelerates along the considered trip. Parameters B_0, B_1, and B_2 consider train type specific characteristics and parameter g = 9.81 m/s^2 is the gravitational acceleration.

$$\overset{[kJ/ton\cdot km]}{E_2} = \overset{[-]}{B_0} + \overset{[-]}{B_1} \cdot \overset{[m/s]}{v} + \overset{[-]}{B_2} \cdot \overset{[m/s]^2}{v^2} + \frac{\overset{[-]}{n_s + 1}}{\overset{[km]}{d}} \cdot \frac{\overset{[m/s]^2}{v_{max}^2}}{2} + \overset{[m/s^2]}{g} \cdot \frac{\overset{[m]}{h}}{\overset{[km]}{d}} \tag{2}$$

Both, the first model (empirical) and the second model (steady state), estimate the train's energy consumption rate in kJ per ton and kilometer independent of the locomotive or engine type (diesel or electric). For trains hauled by a locomotive with an electric engine, the energy consumption rate can be directly used to estimate the total consumed TTW energy in MJ, see Formula (3). Index $i \in \{1, 2\}$ is used to differentiate between the two models. For trains hauled by a locomotive with a diesel engine, the consumed energy needs to be adjusted for the diesel-electric efficiency. This can be done by either considering the efficiency through the emission factors (Hickman et al., 1999, p. 346, Table F9) or by using a diesel-electric efficiency rate ϵ^{de}. The energy estimate in MJ from the second approach is described by Formula (4).

$$\overset{[MJ]}{E_i^{TTW\ elec.}} = \overset{[\frac{kJ}{ton\cdot km}]}{E_i} \cdot \overset{[ton]}{m_{tl}} \cdot \overset{[km]}{d} \cdot 10^{-3}, \; \forall\, i \in \{1, 2\} \tag{3}$$

$$E_i^{TTW\ diesel}{}^{[MJ]} = E_i^{TTW\ elec.}{}^{[MJ]} \cdot \frac{1}{\epsilon^{de}}{}^{[-]}, \ \forall\, i \in \{1,2\} \tag{4}$$

3.2. ARTEMIS

Lindgreen and Sorenson (2005a,b) present an emission estimation model for rail transportation as part of a more comprehensive project on the Assessment and Reliability of Transport Emission Models and Inventory Systems (ARTEMIS). The model is based on a detailed analysis of the physical principles that describe the required energy to move a train. In particular, it estimates the train's energy consumption (in J) by integrating its driving resistance over the traveled distance d, see Formula (5). Thereby, the driving resistance constitutes of rolling resistance F_R, aerodynamic resistance F_L, gradient resistance F_S, and acceleration resistance F_A. Each of these resistances can be calculated from trip and train specific parameters, see Formulas (6) to (9).

$$E_3{}^{[J]} = \int \left(F_R{}^{[N]} + F_L{}^{[N]} + F_S{}^{[N]} + F_A{}^{[N]} \right) \Delta\, d^{[m]} \tag{5}$$

$$F_R{}^{[N]} = C_R{}^{[-]} \cdot m_t{}^{[kg]} \cdot g^{[m/s^2]} \tag{6}$$

$$F_L{}^{[N]} = \frac{1}{2} \cdot \rho^{[kg/m^3]} \cdot C_L{}^{[-]} \cdot A^{[m^2]} \cdot v^{2\,[m/s]^2} \tag{7}$$

$$F_S{}^{[N]} = m_t{}^{[kg]} \cdot g^{[m/s^2]} \cdot \frac{h^{[m]}}{d^{[m]}} \cdot 1000 \tag{8}$$

$$F_A{}^{[N]} = m_t{}^{[kg]} \cdot a^{[m/s^2]} \tag{9}$$

Parameter g = 9.81 m/s^2 is the gravitational acceleration, parameter ρ = 1.2 kg/m^3 is the air density, parameter A is the train's front surface, parameter a is the train's acceleration, and parameters C_R and C_L are train specific rolling and aerodynamic coefficients, respectively. The last two parameters require additional calculations (Kirschstein and Meisel, 2015; Lindgreen and Sorenson, 2005a,b) that are described in Formulas (10) and (11). Here, parameters c_R^{loc}, c_R^{car}, c_1, c_2, c_L^{loc},

and c_L^{car}, are rolling and aerodynamic constants of the considered locomotive and wagons/cars, respectively.

$$\overset{[-]}{C_R} = \overset{[-]}{c_R^{loc}} \cdot \frac{\overset{[t]}{m_{loc}}}{\overset{[t]}{m_t}} + \overset{[-]}{c_R^{car}} \cdot \frac{\overset{[t]}{m_w} \cdot \overset{[-]}{n_w}}{\overset{[t]}{m_t}} + \frac{\overset{[-]}{n_{ax}} \cdot \overset{[-]}{n_w}}{10 \cdot \overset{[t]}{m_t} \cdot \overset{[m/s^2]}{g}} + \overset{[-]}{c_1} \cdot \frac{\overset{[\frac{km}{h}]}{v}}{100} + \overset{[-]}{c_2} \cdot \left(\frac{\overset{[\frac{km}{h}]}{v}}{100} \right)^2 \tag{10}$$

$$\overset{[-]}{C_L} = \overset{[-]}{c_L^{loc}} + \overset{[-]}{c_L^{car}} \cdot \overset{[-]}{n_w} \tag{11}$$

If speed v and acceleration a are constant, the integral from Formula (5) can be solved by using Formula (12). The variables x_1 and x_2 describe the distance of this (constant) speed-acceleration section, i.e., speed v and acceleration a do not change here. For example, considering a trip with a total distance of 750 meters: if a train travels with $v = 50$ km/h and $a = 0.2$ m/s^2 for first 500 meters, then, $x_1 = 0$ and $x_2 = 500$ for this first section, and, if the train travels with $v = 100$ km/h and $a = 0.1$ m/s^2 on the following 250 meters, then, $x_1 = 500$ and $x_2 = 750$ for the second section.

$$\overset{[J]}{E_3} = (\overset{[N]}{F_R} + \overset{[N]}{F_L} + \overset{[N]}{F_S} + \overset{[N]}{F_A}) \cdot (\overset{[m]}{x_2} - \overset{[m]}{x_1}) \tag{12}$$

Theoretically, one could split the actual trip into a sufficiently large number of sections with constant speed and acceleration, then calculate the energy per section by Formula (12), and sum up the values of all sections to come up with an estimate of the whole trip's energy. Clearly, this is not a practical approach and, instead, the authors propose a so-called matrix approach. This approach follows a three step process.

Firstly, a train-specific energy matrix is calculated for various speed-acceleration combinations. The authors suggest acceleration intervals of 0.1 m/s^2 (i.e., $C = \{0, 0.1, ..., 1\}$) and speed intervals of 10 km/h (i.e., $V = \{0, 10, ..., 140\}$). The energy matrix considers the energy from rolling resistance F_R, aerodynamic resistance F_L, and acceleration resistance F_A. The energy from gradient resistance F_S is not considered in the matrix as it depends on the trip's geographical

			speed interval													
			140 - 130	130 - 120	120 - 110	110 - 100	100 - 90	90 - 80	80 - 70	70 - 60	60 - 50	50 - 40	40 - 30	30 - 20	20 - 10	10 - 0
acceleration interval	0.9	1.0	0.00	0.00	0.00	0.00	0.00	0.00	0.00	0.00	0.00	0.00	0.00	0.00	0.00	0.00
	0.8	0.9	0.00	0.00	0.02	0.00	0.00	0.00	0.00	0.00	0.04	0.01	0.02	0.01	0.00	0.00
	0.7	0.8	0.00	0.00	0.00	0.00	0.00	0.00	0.00	0.00	0.00	0.00	0.00	0.00	0.00	0.00
	0.6	0.7	0.00	0.00	0.00	0.00	0.00	0.00	0.00	0.00	0.00	0.00	0.00	0.00	0.00	0.00
	0.5	0.6	0.00	0.00	0.17	0.09	0.07	0.02	0.00	0.05	0.03	0.00	0.01	0.00	0.00	0.00
	0.4	0.5	0.00	0.00	0.08	0.02	0.02	0.12	0.12	0.07	0.06	0.05	0.01	0.01	0.00	0.00
	0.3	0.4	0.05	0.05	0.00	0.00	0.00	0.00	0.00	0.05	0.00	0.00	0.00	0.00	0.00	0.00
	0.2	0.3	0.09	0.19	0.47	0.31	0.35	0.35	0.35	0.09	0.09	0.11	0.11	0.05	0.04	0.00
	0.1	0.2	0.71	1.23	0.76	0.92	0.71	0.64	0.59	0.47	0.29	0.37	0.22	0.11	0.03	0.01
	0.0	0.1	11.49	12.30	9.80	4.25	2.55	1.44	0.00	0.50	0.79	0.17	0.57	0.38	0.20	0.01

Figure 2: Spatial distribution of speed-acceleration combinations of train GP7523 between Glostrup (DK) and Fredericia (DK) (Lindgreen and Sorenson, 2005b).

characteristics (slope profile) and not on the train's acceleration or speed. Instead, the authors suggest to calculate it for the whole trip in the third step of the matrix approach.

Secondly, a trip-specific distribution matrix is determined for all considered speed-acceleration combinations. The authors propose to either use a spatial distribution matrix, indicating the train's traveled distance in each speed-acceleration interval, or a temporal distribution matrix, indicating the train's traveled time in each speed-acceleration interval. Figure 2 shows the spatial distribution matrix of the exemplary train GP7523 between the cities of Glostrup (DK) and Fredericia (DK), which the authors derive from analyzing empirical data. For example, the value 11.49% (bottom left corner) states the share of the distance where the considered train traveled with an acceleration between 0 and 0.1 m/s^2 and a speed between 130 and 140 km/h. The authors suggest to use only those sections of the trip where the train accelerates ($a \geq 0$). For the exemplary train GP7523, this is the case for 55.36 % and 57.61 % of its distance and time, respectively. Note that, by doing so, potential energy gains from regenerative braking are not considered here.

Finally, in a third step, the train-specific energy matrix and the trip-specific distribution matrix are combined in order to estimate the energy of a specific train on a specific trip. This is done in Formula (13). The first part of the formula combines the two matrices: for a matrix element (i, j) ($i \in C,\ j \in V$), e_{ij} describes the value of the energy matrix (F_R, F_L, and F_A) and p_{ij} describes the value of the distribution matrix. The second part of the formula calculates the energy from the gradient resistance (F_S).

$$\overset{[J]}{E_3} = \overset{[m]}{d} \cdot \sum_{i \in C, j \in V} \overset{[N]}{e_{ij}} \cdot \overset{[-]}{p_{ij}} + \overset{[m]}{d} \cdot \overset{[N]}{F_S} \tag{13}$$

Energy E_3 is the kinetic energy that is required to move the train. The train's efficiency is then used to convert this energy to the actual energy demand of the train. Formulas (14) and (15) state the estimated TTW energy in MJ for trains' hauled by electric and diesel locomotives, respectively. Here, ϵ^e and ϵ^d are the corresponding efficiency rates of the locomotive's engine.

$$\overset{[MJ]}{E_3^{TTW\ elec.}} = \overset{[J]}{E_3} \cdot \frac{\overset{[-]}{1}}{\epsilon^e} \cdot 10^{-6} \tag{14}$$

$$\overset{[MJ]}{E_3^{TTW\ diesel}} = \overset{[J]}{E_3} \cdot \frac{\overset{[-]}{1}}{\epsilon^d} \cdot 10^{-6} \tag{15}$$

3.3. EcoTransIT World

The EcoTransIT World (ETW) calculator presents a methodology to estimate emissions for the transport of goods between two locations (EcoTransIT World Initiative, 2019). Thereby, the model considers modes truck, train, airplane, sea ship, and barge as well as transshipment operations between the modes. The results from the ETW model are in accordance with European norm DIN EN 16258 (2012) and the GLEC Framework (Smart Freight Centre, 2020). An implementation of the model is available online at www.ecotransit.org. This website also provides a detailed description of the methodology as well as regular updates of the used parameters and functions.

For rail transportation with electric locomotives, the ETW model uses an empirical function to estimate the specific energy consumption per gross ton and kilometer, see Formula (16). The authors recommend to use the function for trains with a gross load of at most $m_t = 2,200$ t and to use a constant value of 10 Wh/ton·km for larger trains ($m_t > 2,200$ t). The parameter s captures the slope profile of the trip: $s = 0.9$ in flat terrain, $s = 1.0$ in hilly terrain, and $s = 1.1$ in mountainous terrain.

$$\overset{[Wh/ton\cdot km]}{E_4} = 1200 \cdot \overset{[ton]}{m_t}^{-0.62} \cdot \overset{[-]}{s} \tag{16}$$

To convert the energy consumption per gross ton and kilometer to an energy consumption per net ton and kilometer, the model uses a so-called net-gross relation r. This parameter r considers the train's capacity utilization c, the wagon's empty weight m_{we}, and the wagon's max. load m_{wm}, see Formula (17).

$$\overset{[-]}{r} = \frac{\overset{[-]}{c}}{\overset{[-]}{c} + \overset{[t]}{m_{we}} \,/\, \overset{[t]}{m_{wm}}} \tag{17}$$

The capacity utilization c is calculated by considering the train's load factor l as well as the train's empty trip factor e, see Formula (18). The load factor l is the ratio of the wagon's payload to the wagon's capacity (m_{wl}/m_{wm}) and the empty trip factor e is the ratio of the empty traveled distance to the loaded traveled distance (d_{empty}/d_{loaded}). If empty trips are not considered, the train's load factor l is equal to the train's capacity utilization c, i.e., $(d_{empty} = 0) \implies (c = l)$.

$$\overset{[-]}{c} = \frac{\overset{[-]}{l}}{1 + \overset{[-]}{e}} \tag{18}$$

Remember that the energy estimate E_4 is based on empirical observations of an electric train. However, the authors argue that this functional relationship can also be used to estimate the energy from trains hauled by a diesel locomotive, simply by using the diesel-electric efficiency ϵ^{de}. The TTW energy in MJ is then estimated by Formula (19) for electric trains and by Formula (20) for diesel trains.

$$\overset{[MJ]}{E_4^{TTW\ elec.}} = \frac{\overset{[-]}{1}}{r} \cdot \overset{[\frac{Wh}{ton\cdot km}]}{E_4} \cdot \overset{[ton]}{m_{tl}} \cdot \overset{[km]}{d} \cdot 3.6 \cdot 10^{-3} \tag{19}$$

$$\overset{[MJ]}{E_4^{TTW\ diesel}} = \overset{[MJ]}{E_4^{TTW\ elec.}} \cdot \frac{\overset{[-]}{1}}{\epsilon^{de}} \tag{20}$$

3.4. Mesoscopic model

Kirschstein and Meisel (2015) propose the Mesoscopic model to estimate emissions from road and rail freight transportation. The Mesoscopic model combines physical principles from microscopic models, such as the ARTEMIS model, with empirical data from macroscopic models, such as the ETW model. With this, the authors claim to provide a model that combines 'the preciseness of micro-models while requiring only little more information than macro-models' (Kirschstein and Meisel, 2015, p. 13).

The Mesoscopic model is based on the same physical principles that are also used in the ARTEMIS model, see Section 3.2. Thereby, the authors use W-equivalent formulations of the resistances. In particular, the power to overcome air resistance p^{air}, rolling resistance p^{roll}, and gradient resistance p^{grade} are calculated by Formulas (21) to (23). Here, parameters c^{air} and c^{roll} are train specific coefficients for the estimation of aerodynamic and rolling resistances, respectively. For these parameters, the Mesoscopic model uses the calculation methods from the ARTEMIS model ($c^{air} \Leftrightarrow C_L$, $c^{roll} \Leftrightarrow C_R$), see Formulas (10) and (11).

$$\overset{[kW]}{p^{air}} = \frac{1}{2000} \cdot \overset{[-]}{c^{air}} \cdot \overset{[kg/m^3]}{\rho} \cdot \overset{[m^2]}{A} \cdot \overset{[m/s]^3}{v^3} \tag{21}$$

$$\overset{[kW]}{p^{roll}} = \overset{[-]}{c^{roll}} \cdot \overset{[t]}{m_t} \cdot \overset{[m/s^2]}{g} \cdot \overset{[m/s]}{v} \tag{22}$$

$$\overset{[kW]}{p^{grade}} = \overset{[t]}{m_t} \cdot \overset{[m/s^2]}{g} \cdot \overset{[m/s]}{v} \cdot \frac{\overset{[m]}{h}}{\underset{[m]}{d}} \tag{23}$$

Remember that the ARTEMIS model uses the matrix-approach to consider the energy consumption at different speed-acceleration combinations. In contrast to this, the Mesoscopic model uses an approximation function to estimate the energy from acceleration processes. Specifically, the authors propose Function (24) to estimate the energy from acceleration processes W^{inert}_{train}, which considers the train's total weight m_t and the train's average speed v. The authors show

that W_{train}^{inert} describes a good fit for a freight train's acceleration energy that is required for a single acceleration process up to speed v.

$$\overset{[kWh]}{W_{train}^{inert}} = \frac{0.52}{2 \cdot 3600} \overset{[t]}{m_t} \cdot \left(\overset{[m/s]}{v} \right)^2 \tag{24}$$

The Mesoscopic model uses this approximation to estimate the trip's acceleration energy, which is less data demanding compared to the matrix approach used in the ARTEMIS model. In particular, Formula (25) then estimates the train's total energy by considering the required energy to overcome air, rolling, gradient, and acceleration resistance. For the acceleration resistance, the required energy for a single acceleration processes (W_{train}^{inert}) is multiplied with the total number of accelerations $(n^{acc} \cdot d)$ along the route. In this context, n^{acc} is the average number of acceleration processes per kilometer $(n^{acc} = (n_s + 1)/d)$ and serves to reflect different traffic conditions.

$$\overset{[kWh]}{E_5} = \frac{\overset{[km]}{d}}{\underset{[km/h]}{v}} \cdot \left(\overset{[kW]}{p^{air}} + \overset{[kW]}{p^{roll}} + \overset{[kW]}{p^{grade}} \right) + \overset{[-]}{n^{acc}} \cdot \overset{[km]}{d} \cdot \overset{[kWh]}{W_{train}^{inert}} \tag{25}$$

Like in the ARTEMIS model, this energy estimate is the kinetic energy to move the train and the actual energy demand depends on the engine type. This is considered through efficiency rates ϵ^e (electric locomotive) and ϵ^d (diesel locomotive), see Formulas (26) and (27).

$$\overset{[MJ]}{E_5^{TTW\ elec.}} = \overset{[kWh]}{E_5} \cdot \frac{\overset{[-]}{1}}{\epsilon^e} \cdot 3.6 \tag{26}$$

$$\overset{[MJ]}{E_5^{TTW\ diesel}} = \overset{[kWh]}{E_5} \cdot \frac{\overset{[-]}{1}}{\epsilon^d} \cdot 3.6 \tag{27}$$

4. Experiments

The purpose of the experiments is to demonstrate the impact of common train and trip parameters on the estimated emissions of the considered models. In particular, the experiments analyze the impact of varying values of a train's number of wagons, the payload per wagon, the average speed, the trip distance, the number of stops, and the altitude profile along the route. Table 2 shows the range within which these parameters are varied, their default values (which represent a typical freight train in Germany, see FIS (2020)), and whether these parameters are explicitly considered by the models as inputs, or not. The analysis of each parameter's impact helps in understanding each model's methodology. Further, by using such a wide range of values for the varied parameters, the results of the experiments provide estimates of emission rates for various transport scenarios. The model and simulation parameters that are used in the experiments are described in Section 4.1 and the results are described in Sections 4.2 to 4.7.

4.1. Model and simulation parameters

The experiments cover trains that are either hauled by a locomotive with an electric engine or by a locomotive with a diesel engine. For both cases, a six-axle locomotive (frontal area $A = 10$ m^2, locomotive weight $m_{loc} = 123$ t) is assumed to carry a varying number of wagons of the type 'sgis 716' ($n_{ax} = 4$ axles, empty weight $m_{we} = 23$ t, maximal load $m_{wm} = 61$ t). It is assumed that each wagon is loaded with three 20-ft containers, that each wagon's payload m_{wl} includes the empty weight of the containers, and that each wagon's payload m_{wl} is equally distributed

Table 2: Train and trip parameters that are varied in the experiments.

					considered in the model? [a]				
nr	parameter	unit	range	default	1	2	3	4	5
train									
1	number of wagons n_w	-	2-42	20	-	-	√	√	√
2	payload per wagon m_{wl}	t	10-62	38	-	-	√	√	√
3	average speed v	km/h	40-140	90	√	√	(-)	-	√
trip									
4	distance d	km	40-440	240	√	√	√	-	√
5	number of stops n_s	-	1-5	2	√	√	(-)	-	√
6	altitude difference h	m	0-400	200	-	√	√	√	√

[a] 1: MEET (empirical), 2: MEET (steady state), 3: ARTEMIS, 4: ETW, 5: Mesoscopic

among all containers. The efficiency of diesel and electric trains is set to $\epsilon^d = 0.35$ and $\epsilon^e = 0.65$ (Lindgreen and Sorenson, 2005b, p. 27), respectively, and the diesel-electric efficiency is set to $\epsilon^{de} = 0.37$ (EcoTransIT World Initiative, 2019, p. 63).

For the energy estimate with the empirical MEET model (E_1), the parameters A_0 and A_1 correspond to a large freight train with an empty mass of 600 t and are set to 63 and 0.019 (Hickman et al., 1999, p. 223), respectively. Furthermore, it is assumed that stops n_s are uniformly distributed across the trip such that the distance between any two consecutive stops is the same, i.e., $d_s = d/(n_s + 1)$. For the MEET's energy estimate that is based on the train's steady state loading (E_2), it is assumed that the maximal speed v_{max} is a multiple of the average speed v ($v_{max} = 1.5 \cdot v$) and that $B_0 = 24.7$, $B_1 = 0$, and $B_2 = 0.0845$ (Hickman et al., 1999, p. 223).

The matrix approach of the ARTEMIS model is used with the spatial distribution of the freight train between Glostrup and Fredericia, see Figure 2. Clearly, this causes misleading emission rates in the experiments as the distribution matrix is based on a specific freight train in Denmark, e.g., whose total payload is only 126 tons whereas it is 760 tons for this study's default train. However, using appropriate speed-accelerations for each experimental setting requires a vast amount of detailed real-world rail freight data. The issue of data availability is discussed in more detail in Section 5. The following values are used to calculate the train specific rolling and aerodynamic coefficients C_R and C_L that are used in the ARTEMIS and Mesoscopic model: $c_R^{car} = 0.0006$, $c_R^{loc} = 0.004$, $c_1 = 0.0005$, $c_2 = 0.0006$, $c_L^{loc} = 1.1$, and $c_L^{car} = 0.218$ (Lindgreen and Sorenson, 2005a, p. 7-8, 29).

The ETW model uses parameter s to consider the slope profile of the trip. In the experiments, the altitude difference h between the origin location and the destination location is used as a proxy for s. In particular, it is assumed that $s = 0.9$ for altitude differences below 100 meters ($h < 100$), $s = 1.0$ for altitude difference between 100 and 300 meters ($100 \leq h \leq 300$), and $s = 1.1$ for altitude differences of more than 300 meters ($h > 300$). Empty trips are not considered in the experiments, e.g., $d_{empty} = 0$ and $d_{loaded} = d$.

As explained in Section 2, energy and emission factors can be used to convert a TTW energy estimate (E^{TTW}) to a WTW emission estimate (G^{WTW}), see Figure 1. For trains hauled by electric locomotives, the emission factor resulting from the EU-28 average energy supply is used, i.e.,

g^{WTW} = 137 gCO_2e/MJ (EcoTransIT World Initiative, 2019, Tab. 52), and for trains hauled by locomotives that generate their power from diesel fuel, the emission factor resulting from a 7% bio-diesel is used, i.e., g^{WTW} = 88.21 gCO_2e/MJ (DIN EN 16258, 2012, Tab. A.4). For both train types, total WTW emissions are calculated with Formula (28).

$$\overset{[gCO_2e]}{G^{WTW}} = \overset{[MJ]}{E^{TTW}} \cdot \overset{[gCO_2e/MJ]}{g^{WTW}} \tag{28}$$

In the following sections, experimental results are mainly presented in terms of WTW emission rates r in $gCO_2e/ton{\cdot}km$. These rates are computed by dividing total emissions G^{WTW} by the train's payload m_{tl} and the trip's distance d, see Formula (29).

$$\overset{[gCO_2e/ton\cdot km]}{r} = \frac{\overset{[gCO_2e]}{G^{WTW}}}{\overset{[t]}{m_{tl}} \cdot \overset{[km]}{d}} \tag{29}$$

4.2. Number of wagons

Figure 3 shows the WTW emission rate r for a train with a varying number of wagons n_w. Results are presented for a train that is hauled by a diesel locomotive (Figure 3a) and for a train that is hauled by an electric locomotive (Figure 3b). It can be seen that an increasing number of wagons leads in all models other than MEET and under both engine types to degressive emission rates. In other words, the emission rate decreases with a larger number of wagons at a decreasing marginal rate. This is because some of the train's total emissions are fix and independent of the number of wagons, such as the emissions caused from moving the locomotive. Thus, since total emissions are equally distributed over the train's total payload in emission rate r, each additional wagon decreases the share of 'wagon-independent' emissions per payload and ton. In contrast, the MEET models already estimate a rate per (loaded) ton and kilometer, which makes their estimated emission rates independent of a varying number of wagons.

Remember that all of the considered models estimate an energy demand that is somehow independent of the engine type. Thus, differences between diesel and electric locomotives arise from energy factors, emission factors, and efficiency rates, which are assumed to be equal in all models and for all experiments. For each model, this leads to a similar pattern of emission rates for both

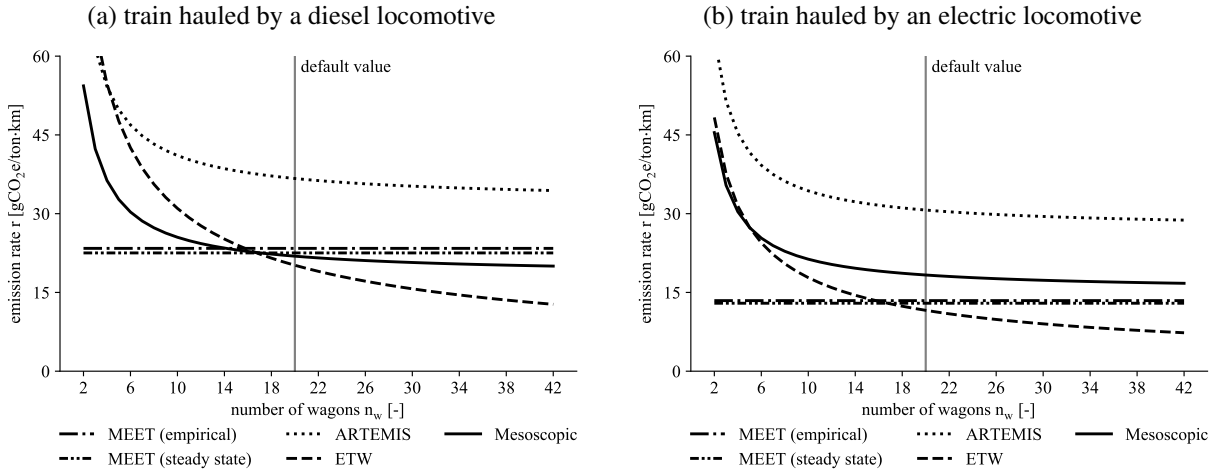

Figure 3: WTW emission rate r for a varying number of wagons n_w.

engine types. This is why the following sections concentrate on results solely for one engine type, namely diesel.

4.3. Payload per wagon

Figure 4 shows the train's WTW emission rate r (Figure 4a) and the train's TTW energy E^{TTW} (Figure 4b) for varying values of the payload per wagon m_{wl}. It can be seen that an increasing payload per wagon results in a degressive emission rate in the ARTEMIS, ETW, and Mesoscopic model. The explanation is similar to the one given for a varying number of wagons, see Section 4.2. In particular, an increasing payload per wagon decreases the share of 'payload-independent' emissions, such as the emissions caused from moving the locomotive or the wagon's empty weight, per payload and ton, which leads to degressive emission rates in the models other than MEET. In contrast, energy in the MEET models is already estimated per (loaded) ton and kilometer, which leads to constant emission rates under varying values for the payload per wagon. Total TTW energy E^{TTW} increases with a higher payload per wagon in all models. This increase is linear in the MEET models, the ARTEMIS model, and the Mesoscopic model and almost linear in the ETW model. Note that the 'payload-independent' energy can be easily identified in Figure 4b as it is at $m_{wl} = 0$. As mentioned before, energy estimates are directly linearly related to emission estimates through energy and emission factors, see Figure 1. This is why the following sections

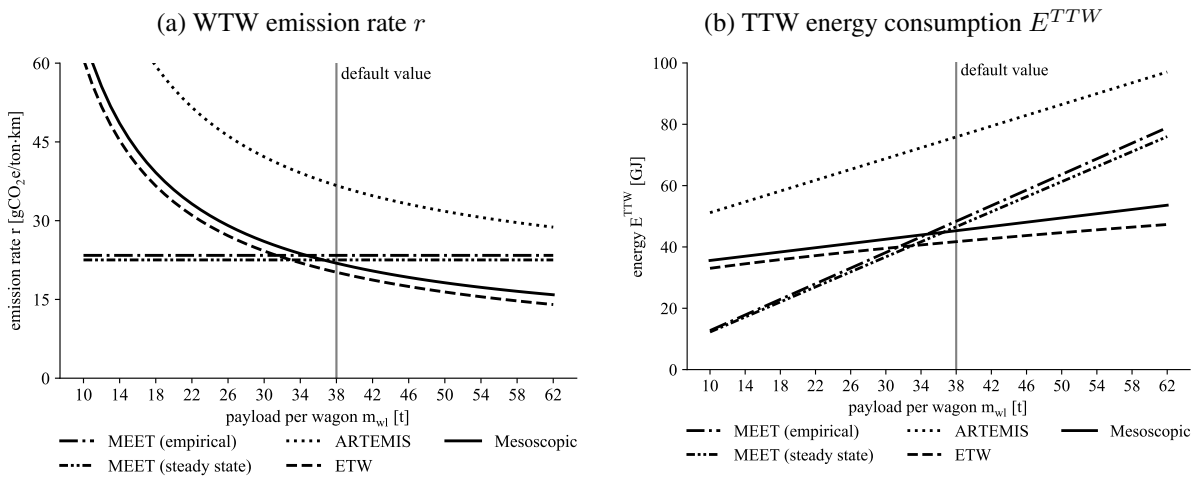

Figure 4: Emission rate and energy consumption for a varying payload per wagon m_{wl} (diesel train).

present results only for the emission rate r. However, all findings also apply to energy measures and the emission values can easily be converted to energy values simply by using the respective energy and emission factors.

4.4. Speed

Figure 5a shows the WTW emission rate r for varying values of the train's average speed v. It can be seen that the average speed has no impact in the ARTEMIS model and the ETW model. For the ARTEMIS model, this is because the same speed-acceleration distribution from Figure 2 is used in all experiments. Clearly, this is unrealistic as different average speeds also result in different speed-acceleration distributions. Yet, it was not possible to find empirical data for all the speed-acceleration intervals that were considered in the experiments. For ETW, average speed has no impact on the emission rate because the ETW energy estimate only depends on the train's total weight and the trip's slope profile, see Formula (16). In contrast, the emission rate estimated with the MEET models or the Mesoscopic model increases quadratically with the average speed. The quadratical increase derives directly from the respective formulas, see Formulas (1) for MEET (empirical), (2) for MEET (steady state), and (24) for the Mesoscopic model.

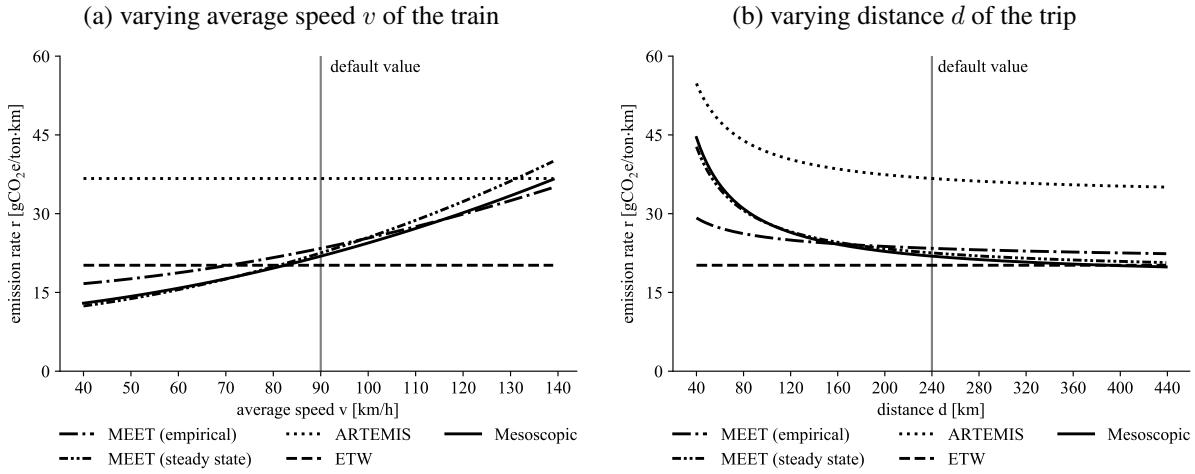

Figure 5: WTW emission rate r for a varying average speed v and a varying distance d (diesel train).

4.5. Distance

Figure 5b shows the WTW emission rate r for varying values of the trip's distance d. As already described in the previous section on the impact of speed, the ETW energy estimate only depends on the train's total weight and the trip's slope profile. Thus, the traveled distance has no impact on the emission rate if it is estimated with the ETW model. For all other models, increasing distance leads to degressive emissions rates. This is because the models incorporate that increasing distance usually leads to fewer acceleration processes per kilometer. Thus, the emissions from acceleration processes become less relevant with increasing distance. Note that emission rates are very high for small distances (e.g., for $d < 80$). The reason for this is that most models are designed for typical train transportation scenarios which involve larger distances. For too short distances, estimates are therefore unrealistic. The empirical MEET model explicitly states that it should only be applied to trips of which the distance between the stops is between 80 and 200 kilometers.

4.6. Number of stops

The number of stops are used to capture the train's energy that results from acceleration processes. Such accelerations are required at the beginning of the trip as well as after each stop. Figure 6a shows that the WTW emission rate r increases with the number of stops in the MEET

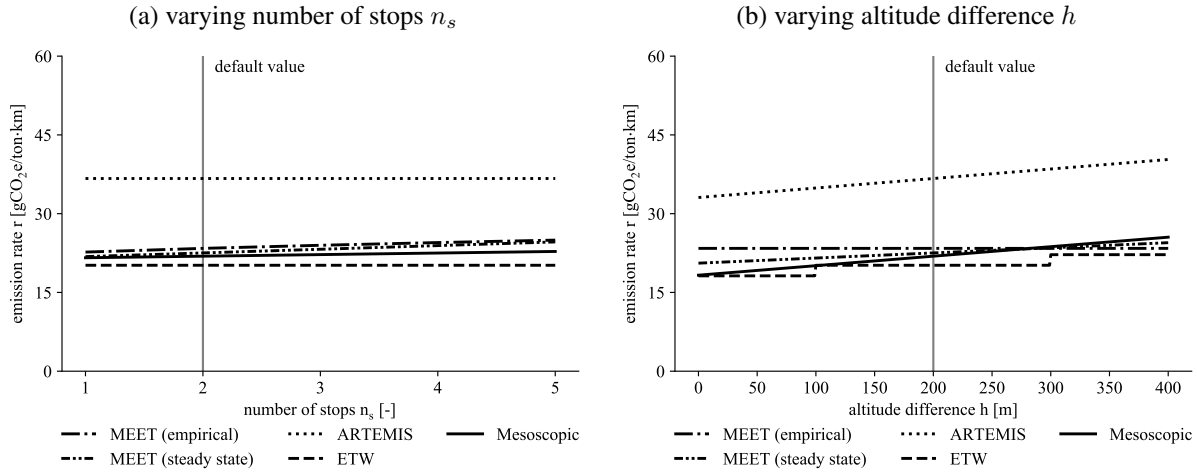

Figure 6: WTW emission rate r for a varying number of stops n_s and a varying altitude difference h (diesel train).

models and in the Mesoscopic model whereas it is constant in the ARTEMIS model and in the ETW model. For the ARTEMIS model, this is because the number of stops are not explicitly considered by the matrix approach. However, the approach implicitly considers the number of acceleration processes through the distribution of speed-acceleration combinations. More precisely, a higher number of stops usually implies a higher probability for intervals of low speed and high accelerations. But, as the same speed-acceleration distribution is used in all experiments, the number of stops has no impact here. The ETW model uses empirical data to estimate the energy and emissions. Similar to speed and distance, the number of stops is not considered as an independent variable which results in a constant emission rate for a varying number of the stops.

4.7. Altitude difference

Finally, Figure 6b shows the impact of the trip's gradient on the WTW emission rate r. There are two ways how the models consider this. Firstly, by using the altitude difference h between the origin and the destination (MEET steady state, ARTEMIS, and Mesoscopic) and secondly, by using slope profile s (ETW). The empirical MEET model does not consider altitudes, which results in constant emission rates. In contrast, increasing altitude differences result in continuously increasing emission rates in the MEET model (steady state), in the ARTEMIS model, and in the Mesoscopic model, whereas they result in discontinuously increasing emission rates in the ETW

model. The last is because slope profile s is assumed to change at pre-defined altitude differences of $h = 200$ and $h = 400$ meters. Note that only positive changes (uphill) are considered in this experiment. However, the reverse results arise for downhill slopes. This is because the considered models do not differentiate between the direction (sign) of the slope which implicitly assumes a total recovery of the uphill consumed energy when going downhill again. Heinold and Meisel (2018) suggest using an adjusted variant for the slope that only considers parts of the recovered energy from negative slopes.

5. Selecting an appropriate model

As there exist numerous models for estimating emissions, it is a challenging task to select an appropriate model for a specific transport scenario, especially, as the availability of data often limits the choice of applicable models. For example, whereas a train's traveled distance might be known (or can be calculated from public sources), its actual speed and acceleration profile is often unknown. Some models, such as ETW, therefore concentrate on input factors that are easy to collect, e.g., a train's total weight. The experiments in the previous section have shown which input factors are most relevant to each of the models. Figure 7 sums up the results. The figure shows the impact of the train's number of wagons (row 1), the train's payload per wagon (row 2), the train's speed (row 3), the trip's distance (row 4), the trip's number of stops (row 5), and the trip's altitude difference (row 6) on each model's emission estimate (column 1 to 5). In contrast to Table 2, which indicates whether those parameters are considered in a model, or not, Figure 7 makes it easy to spot how they are captured in a model's emission rate. For example, looking at the ETW model (column 4), the emission rate decreases with an increasing number of wagons or payload per wagon, it remains constant for variations in speed, distance, or number of stops, and it discontinuously increases with increasing altitude differences. Similarly, for a specific parameter, it is easy to identify the parameter's impact on each model's emission rate. For example, looking at the row of parameter speed (row 3), it can be seen that the emission rate quadratically increases if it is estimated with the MEET models or the Mesoscopic model, whereas the emission rate is constant if it is estimated with the ARTEMIS model or the ETW model. However, the same speed-acceleration matrix is used in the ARTEMIS model, even for the experiments that vary speed and

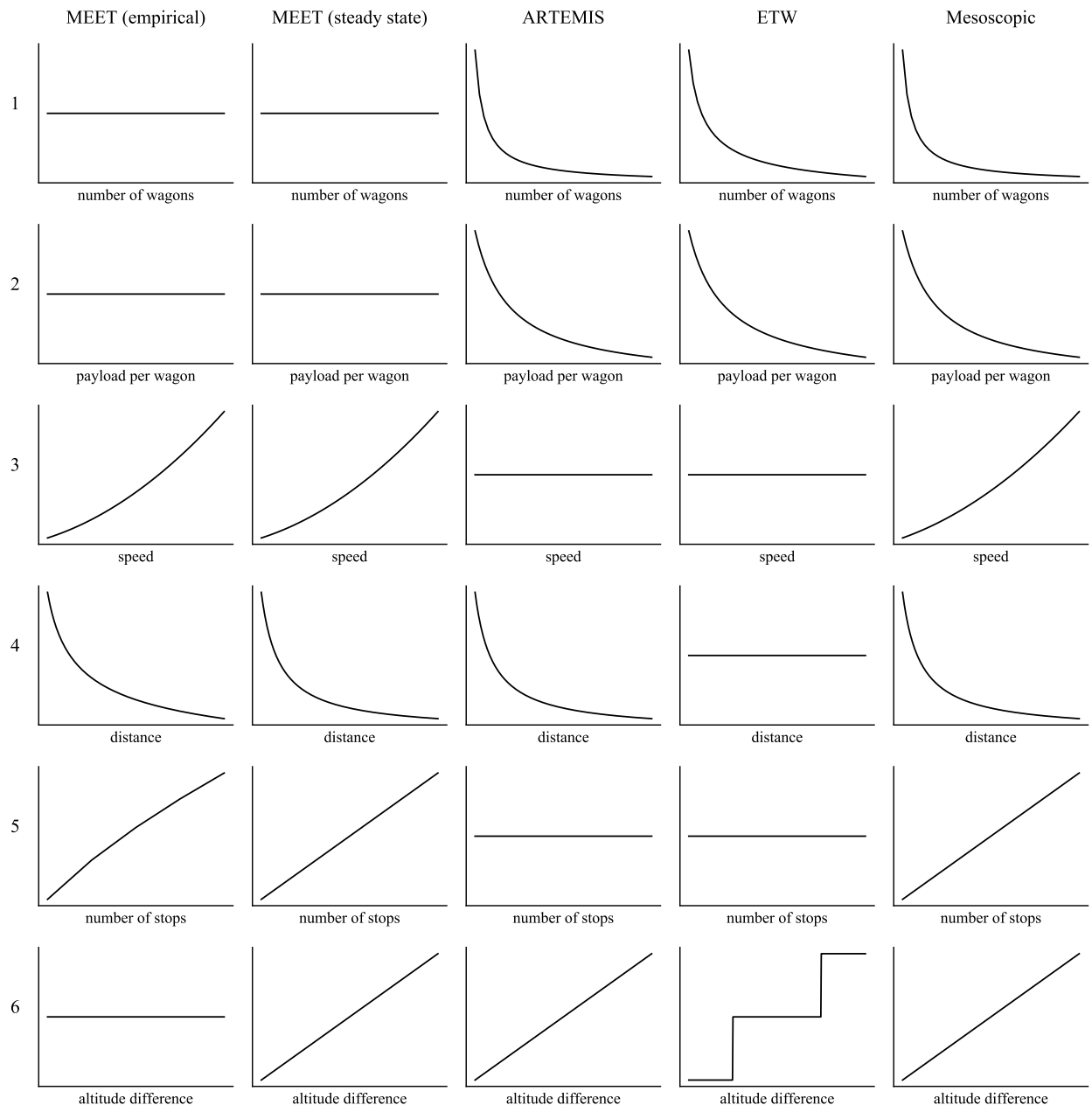

Figure 7: Impact of varying train and truck parameters (rows) on each model's WTW emission rate (columns).

number of stops.

In addition to these common trip and train parameters, all of the models considered in this paper use some kind of statistical parameters or functions, such as a train's physical resistances, to estimate emissions. The availability of up-to-date values for these parameters might be another key consideration, especially, as regular updates might be required due to technological advancements.

Overall, some models need only a few data inputs but generate quite coarse results. These models might still be useful in a rail project proposal or feasibility analysis. On the contrary, other models might be more preferred in detail design phases when the alignment of the transport scenario is almost determined, which might be the case for shippers or logistics service provider.

Anyhow, even with all input data available to apply the models, it is not possible to tell which of the models results in the 'best' estimate, as the 'true' emissions require an actual measurement of emissions. For example, the diesel default train used in the experiments results in emission rates of 20.17, 21.90, 22.52, and 23.39 gCO_2e/ton·km using the ETW, Mesoscopic, MEET (steady state), and MEET (empirical) model, respectively. While these estimates are similar to each other as well as similar to other estimates found in the literature, e.g., the Network for Transport Measures (2018) reports average emission rates of 23 gCO_2e/ton·km for diesel freight trains in the EU, it is not possible to say which of the models is absolutely better than another. Furthermore, the experiments in Section 4 have demonstrated that differences between the models might be significantly higher for other transport scenarios. Thus, it might not be reasonable to exclusively use one or another model, but, instead, use several models covering different aspects of the considered train and trip.

6. Conclusion

This paper has reviewed five emission estimation models for rail freight transportation. In particular, two models from the MEET project, the ARTEMIS model, the ETW model and the Mesoscopic model have been considered. These models quantity emissions by estimating a train's tank-to-wheel energy consumption. For this, the models use train and trip specific parameters that have been described in detail in this paper. Engine type specific energy and emission factors are then used to convert energy estimates into emission estimates.

An computational study has analyzed the impact of relevant parameters on the estimated emissions. In particular, results have been presented for varying values of a train's number of wagons, the payload per wagon, the average speed, the trip distance, the number of stops, and the altitude profile along the route. The analysis has shown that the parameters impact on the well-to-wheel emission rate (gCO_2e/ton·km) is considered differently in the five models: increasing number of

wagons or payloads per wagon lead to a degressive emission rate in three models and have no impact on the emission rate in two models, increasing speed increases the emission rate in three models and has no impact on the emission rate in two models, increasing distance decreases the emission rate in four models and has no impact on the emission rate in one model, an increasing number of stops increases the emission rate in three models and has no impact on the emission rate in two models, and an increasing altitude difference increases the emission rate in four models and has no impact on the emission rate in one model. This study has also discussed transport scenarios in which each of the models can be applied to. Here, the availability of data plays a vital role as some models require a substantial amount of specific input data, such as technical parameters about the locomotive. Despite of this, it has been shown that the models lead to similar estimates for a realistic default train. Overall, is has been shown that it is the considered transport scenario that decides which model is most appropriate to estimate emissions from rail freight transportation.

This study has concentrated on the most prominent parameters but did not vary all possible parameters. For example, the rolling and aerodynamic coefficients (used in the ARTEMIS and Mesoscopic model) have not been varied in the experiments, although they can have a significant impact on the estimated energy/emissions. However, a proper setting of these parameters is challenging as they depend on, for example, train-type specific characteristics, and it would be interesting to provide an overview of these parameters for several common train-types. The matrix approach of the ARTEMIS model uses trip-specific distribution matrices to capture realistic speed-acceleration combinations. The same distribution from a freight train in Denmark has been used throughout the experiments. It is left for future research to collect real data for trains' driving cycles in order to build distribution matrices for additional transportation scenarios. Finally, Hickman et al. (1999) and Lindgreen and Sorenson (2005a,b) already provide some findings on the actual emissions that are emitted by a freight train. It would be interesting to update and extend these results and, for example, to investigate the impact of technological improvements on the emitted emission.

Acknowledgments

This research was supported by the German Research Foundation (DFG) under references ME 3586/1-1 and ME 3586/1-2. Special thanks go to three anonymous reviewers for their valuable

comments which helped to improve the manuscript considerably.

Appendix A. Python scripts

The Python code with the implementations of the emission estimation models are available as additional files in the electronic appendix of this paper. These scripts can be used to reproduce all results from the experimental study. They can also be used for performing own calculations. All data and material is also available from the corresponding author on request.

Bibliography

Craig, A. J., Blanco, E. E., Sheffi, Y., 2013. Estimating the CO2 intensity of intermodal freight transportation. Transportation Research Part D: Transport and Environment 22, 49–53.

de Miranda Pinto, J. T., Mistage, O., Bilotta, P., Helmers, E., 2018. Road-rail intermodal freight transport as a strategy for climate change mitigation. Environmental Development 25, 100–110.

Demir, E., Bektaş, T., Laporte, G., 2011. A comparative analysis of several vehicle emission models for road freight transportation. Transportation Research Part D: Transport and Environment 16 (5), 347–357.

DIN EN 16258, 2012. Methodology for calculation and declaration of energy consumption and GHG emissions of transport services (freight and passengers).

EcoTransIT World Initiative, 2019. Ecological Transport Information Tool for Worldwide Transports. Methodology and Data. Update 2019. https://www.ecotransit.org/download/EcoTransIT_World_Methodology_Data_Update_2019.pdf (visited on 20.06.2020).

Eurostat, 2020. Greenhouse gas emission statistics - emission inventories. https://ec.europa.eu/eurostat/statistics-explained/index.php?title=Greenhouse_gas_emission_statistics_-_emission_inventories (visited on 20.06.2020).

FIS, 2020. Forschungs-Informations-System: Betriebstechnische Grenzparameter für Güterzüge. https://www.forschungsinformationssystem.de/servlet/is/324625/ (visited on 20.06.2020).

GHG Protocol, 2020. The greenhouse gas protocol: A corporate accounting and reporting standard. https://ghgprotocol.org/sites/default/files/standards/ghg-protocol-revised.pdf (visited on 20.06.2020).

Heinold, A., Meisel, F., 2018. Emission rates of intermodal rail/road and road-only transportation in Europe: A comprehensive simulation study. Transportation Research Part D: Transport and Environment 65, 421–437.

Heinold, A., Meisel, F., 2019. Emission oriented vs. time oriented routing in the european intermodal rail/road freight transportation network. In: Bierwirth, C., Thomas, K., Sackmann, D. (Eds.), Logistics Management. Lecture Notes in Logistics. Springer, pp. 188–202.

Hickman, J., Hassel, D., Joumard, R., Samaras, Z., Sorenson, S., 1999. Methodology for calculating transport emissions and energy consumption. https://trimis.ec.europa.eu/sites/default/files/project/documents/meet.pdf (visited on 20.06.2020).

International Energy Agency, 2019. The future of rail: Opportunities for energy and the environment. https://www.iea.org/reports/the-future-of-rail (visited on 20.06.2020).

International Transport Forum, 2019. ITF Transport Outlook 2019. https://doi.org/10.1787/transp_outlook-en-2019-en (visited on 20.06.2020).

IPPC, 2018. Global warming of 1.5°C. https://www.ipcc.ch/site/assets/uploads/sites/2/2019/06/SR15_Full_Report_High_Res.pdf (visited on 20.06.2020).

Kirschstein, T., Meisel, F., 2015. GHG-emission models for assessing the eco-friendliness of road and rail freight transports. Transportation Research Part B: Methodological 73, 13–33.

Kiyota, A. S., Yoshizaki, H. T. Y., Massara, V. M., 2015. Analysis of greenhouse gases in the emissions of Brazilian freight transport. International Journal of Low-Carbon Technologies 10 (4), 438–440.

Lindgreen, E. B. G., Sorenson, S. C., 2005a. Driving resistance from railroad trains. Tech. rep., Technical University of Denmark. Department of Mechanical Engineering.

Lindgreen, E. B. G., Sorenson, S. C., 2005b. Simulation of energy consumption and emissions from rail traffic. Tech. rep., Technical University of Denmark. Department of Mechanical Engineering.

Moro, A., Lonza, L., 2018. Electricity carbon intensity in European Member States: Impacts on GHG emissions of electric vehicles. Transportation Research Part D: Transport and Environment 64, 5–14.

Network for Transport Measures, 2018. Rail cargo transport baselines 2018. https://www.transportmeasures.org/en/wiki/evaluation-transport-suppliers/rail-cargo-transport-baselines-2017/ (visited on 20.06.2020).

Piecyk, M., Cullinane, S., Edwards, J., 2012. Assessing the external impacts of freight transport. In: McKinnon, A., Browne, M., Whiteing, A. (Eds.), Green logistics: Improving the environmental sustainability of logistics, 2nd Edition. Kogan Page Limited London, New York, Ch. 2, pp. 31–50.

Smart Freight Centre, 2020. Global logistics emissions council (GLEC): The global method for calculation and reporting of logistics emissions. https://www.smartfreightcentre.org/en/how-to-implement-items/what-is-glec-framework/58/ (visited on 20.06.2020).

The Times, 2020. Xi's 'silk railway' halves delivery time to europe. https://www.thetimes.co.uk/article/xis-silk-railway-halves-delivery-time-to-europe-wft98n7z6 (visited on 20.06.2020).